



## CFD Simulation of Aerodynamics Truck Using Cylinder as Drag Reduction Device

Ainul Ghurri<sup>1,\*</sup>, Muhamad Alim<sup>1</sup>, Made Nara Pradipta Adi<sup>1</sup>, Satrio Galang Bhuana Putra<sup>1</sup>, Mallory Ekananda Mantik<sup>1</sup>, Sonny Suharto<sup>1</sup>, Rivaldo Anderson<sup>1</sup>

<sup>1</sup> Department of Mechanical Engineering, Engineering Faculty, Universitas Udayana, Kampus Bukit Jimbaran 80361, Badung, Bali Indonesia

### ARTICLE INFO

#### Article history:

Received 2 January 2023  
Received in revised form 8 April 2023  
Accepted 17 April 2023  
Available online 6 May 2023

#### Keywords:

Truck; drag reduction; cylinder; CFD simulation

### ABSTRACT

Reducing drag is an excellent approach to improving truck efficiency and saving fuel. The addition of the cylinder could be an alternative for drag reduction devices like the windshield that has a similar function to enhance the truck's aerodynamic performance. A numerical analysis was performed using Ansys Fluent CFD software to estimate the influence of the cylinder on the truck's drag force. The study was conducted by comparing truck without additional cylinder above the truck's head, truck with windshield, and truck with cylinder variations, which round, type-I, and type-D cylinders. In the simulation, the analysis was carried out at a velocity of 30 m/s using the k-epsilon turbulence model. A grid independence test was conducted to minimize errors and optimize iteration time. The simulation results showed that using round, I-type, and D-type cylinders as an alternative to the windshield reduced the truck's drag coefficient, with the D-type cylinder achieving the highest reduction in drag coefficient, which is 0.72. Modifications in the design of the drag reduction cylinder can lower fuel consumption indirectly by 6.95 % using a D-type cylinder.

## 1. Introduction

Aerodynamics is the study of how moving objects interact with the air [1]. The result of the interaction between a moving vehicle and the air is in the form of downforce, lift force, and aerodynamic drag force. Aerodynamic drag consists of two components: pressure drag and friction drag. Due to the influence of the boundary layer separation and wake region on the rear of the object, pressure drag is closely related to object geometry and provides for more than 80 % of the total drag on the vehicle [2,3]. The location of the boundary layer separation and wake directly becomes an essential factor in determining the value of aerodynamic drag, currently known as the drag coefficient ( $C_D$ ) [4].

The shape of the vehicle body and the airflow velocity will significantly impact the drag coefficient, especially the vehicle body, like a truck with a large cross-sectional area. According to the

\* Corresponding author.

E-mail address: [a\\_ghurri@unud.ac.id](mailto:a_ghurri@unud.ac.id)

<https://doi.org/10.37934/arfmts.105.2.166181>

aerodynamic drag formula, the cross-sectional area was the one that affected the results of the drag force. A larger cross-sectional area means the more the drag force received by the truck when given the fluid's velocity, thus reducing the engine's and fuel's efficiency. A design vehicle such as a truck can be accepted if there is a decrease in the drag coefficient and an increase in stability to increase the efficiency; thereby, researchers often conduct a preliminary analysis using CFD software to assess the aerodynamic [3]. The drag value is heavily influenced by the aerodynamic design of the truck body. Components such as skirts on the sides and boat tails on the back of the truck can be added to reduce drag. By adding this component, research by Praveen *et al.*, [5] and Landman *et al.*, [6] was able to reduce the drag on trucks by 30 %. A windshield can also be added to the top of the truck to reduce drag. According to research conducted by Firman *et al.*, [7] using CFD simulation on the design of trucks with a windshield, adding a windshield can lower the amount of drag on the vehicle. A similar result was found by Charles *et al.*, [8] on trucks that had a windshield deflector added. This component can potentially reduce the truck's drag by 34 %.

The existence of these components is thought to demand high installation costs. One alternative that can be used to replace the windshield to reduce drag is the addition of a cylinder at the front of the truck. According to research by Tsutsui *et al.*, [9], putting a tiny cylinder in front of the main cylinder can reduce drag by up to 63 %. This research also is supported by Gunawan *et al.*, [10], which reveal that the presence of a barrier in the form of a small cylinder can reduce drag on the main cylinder by 64.5 %. The drag will increase as the distance between the small and main cylinders increases due to the location of the flow separation point. The same thing was also conducted by Widodo *et al.*, [11] by adding two circular disturbance bodies at the front of the main cylinder to create a turbulent flow pattern, which delays the flow separation point and reduces drag.

Based on previous research by Gunawan *et al.*, [10] and Yuwono *et al.*, [12], adding a small cylinder in the front of the main cylinder will reduce drag on the main cylinder. Therefore, since no research scrutinized the utilization of the cylinder on the truck, which is potentially used as the drag reduction device. Thus, it is necessary to conduct further preliminary analysis using Ansys Fluent CFD simulation software regarding the application of various type cylinders in aerodynamics to reduce drag on the trucks by mounting the cylinder on the truck head. The purpose of adding this cylinder is to break up the airflow and create a turbulent flow pattern, which delays the separation point in the aerodynamics region.

## 2. Methodology

### 2.1 Design and Computational Method

In this study, the 3D truck model was designed using Autodesk Inventor Student Version 2020. To investigate the truck's aerodynamics, ANSYS 20.2 was used as computational fluid dynamic software by importing the 3D geometry to ANSYS Fluent. ANSYS Fluent was chosen since it uses the cell-centred method as its finite volume method, which has larger degrees of freedom that allows the simulation to run appropriately [12]. ANSYS is used extensively in the simulation of various topics of internal flow such as infusion pump [13], heat transfer of flow in pipes [14,15]; and many topics in external flow of aerodynamic object such as airfoil [16], irregular shape object [17] and wind turbine rotor [18]. ANSYS Fluent is the most common simulation software used in car aerodynamic simulation [19-23]. In general, simulation processes can be classified into three steps: pre-processing, solver, and post-processing. First, pre-processing was a process in which the 3D geometry was designed and imported; subsequently, the meshing process was conducted to the geometry; the mesh quality in this process would also determine the accuracy of the simulation. Secondly, before running the simulation, the boundary condition was adjusted to define the initial condition of the simulation, and

the solution method was selected to assist in the convergence of the simulation. Subsequently, after running the simulation, the solution process should be convergence before evaluating the simulation results. If convergence cannot be obtained, then configurations in the solver stage should be revised. Finally, the post-processing stage can be assessed after the convergence of the solution process. Furthermore, the simulation result was investigated, especially coefficient drag, drag force, velocity contour, and velocity streamline.

### 2.2 Truck Model Geometry

The truck geometry is simplified by the model throughout the simulation process using Ansys Fluent, and the truck dimensions may be shown in Figure 1.

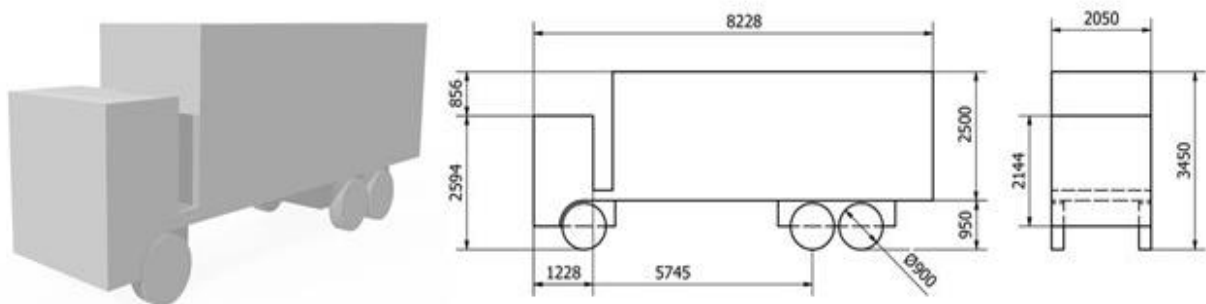


Fig. 1. Truck models without drag reduction in the simulation

In this study, variations in drag reduction were simulated to investigate the effect of adding drag reduction to the value of the drag coefficient and the flow pattern around the truck. Table 1 exhibits the truck's geometry by adding the windshield, the drag reduction cylinder, the D-type drag reduction cylinder, and the I-type drag reduction cylinder. According to Igarashi *et al.*, [16], the ideal cut angle ( $\theta_f$ ) for the D-type cylinder is  $53^\circ$ , and the optimal cut angle ( $\theta_r$ ) for the I-type cylinder is  $127^\circ$  (Figure 2). Since these two types of cylinders have not been utilized to observe the performance of aerodynamics in the truck, this study would harness two types of cylinders as the reference construction to the drag reduction device based on the cylinder.

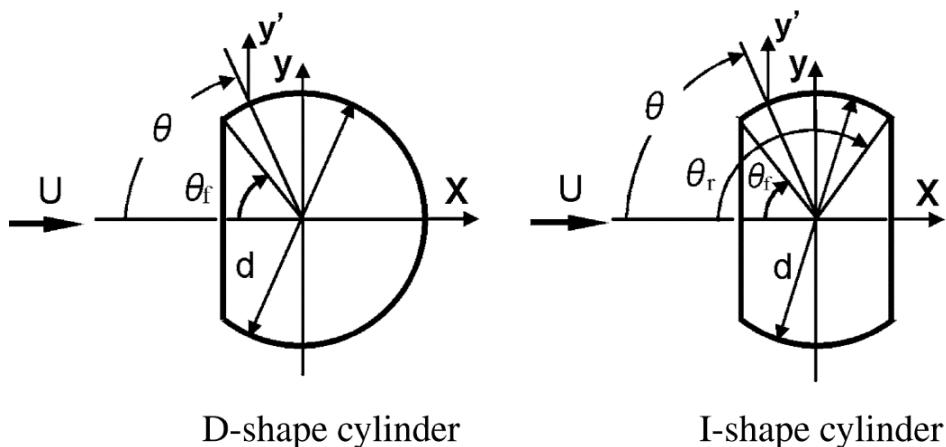
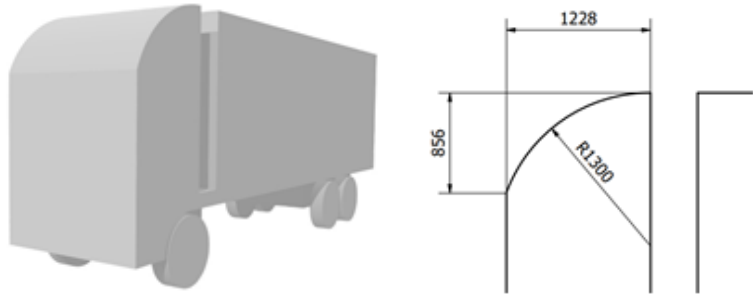
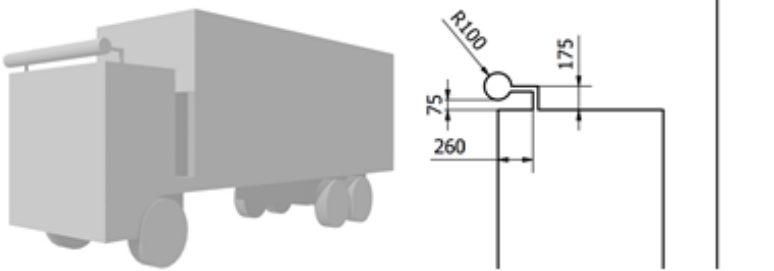
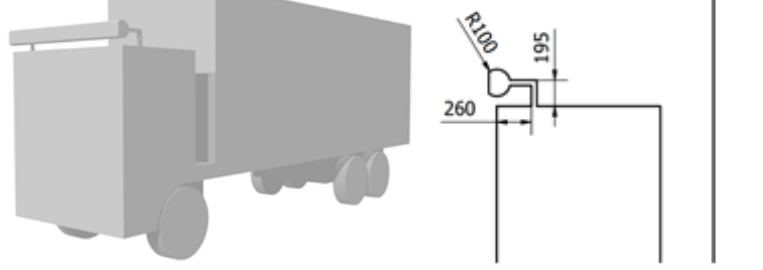
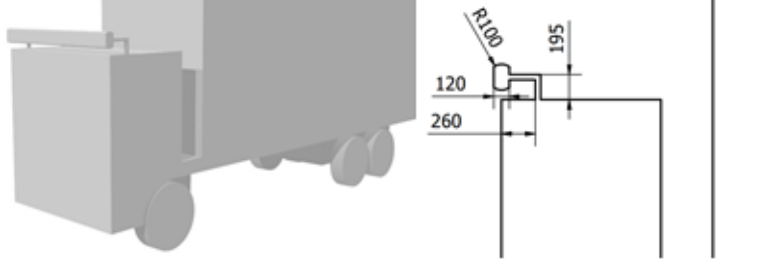


Fig. 2. Type-D and type-I cylinders on research by Igarashi *et al.*, [16]

**Table 1**  
 The variation of the drag reduction devices on the truck

Description	Geometry
Windshield Drag Reduction	
Cylinder Drag Reduction	
Type-D Cylinder Drag Reduction	
Type-I Cylinder Drag Reduction	

### 2.3 Numerical Method

Computational Fluid Dynamics (CFD) is a fluid flow analysis method that uses numerical analysis to solve the Navier-Stokes equation for the movement of each fluid particle [17]. Fluid flow analysis in a model is carried out to analyze fluid particles' movement and behavior in detail, also the fluid's pressure and velocity contours around the model. The basic theory behind the implementation of

CFD analysis is to divide the fluid flow into small cells, and each mesh will be solved using the three-dimensional Navier-Stokes equation as follows [24-26]

Continuity

$$\rho \left( \frac{\partial}{\partial t} + \frac{\partial u}{\partial x} + \frac{\partial v}{\partial y} + \frac{\partial w}{\partial z} \right) = 0 \quad (1)$$

Momentum

$$x: \rho \left( \frac{\partial u}{\partial t} + u \frac{\partial u}{\partial x} + v \frac{\partial u}{\partial y} + w \frac{\partial u}{\partial z} \right) = \nu \left( \frac{\partial^2 u}{\partial x^2} + \frac{\partial^2 u}{\partial y^2} + \frac{\partial^2 u}{\partial z^2} \right) - \frac{\partial p}{\partial x} + f_x \quad (2)$$

$$y: \rho \left( \frac{\partial v}{\partial t} + u \frac{\partial v}{\partial x} + v \frac{\partial v}{\partial y} + w \frac{\partial v}{\partial z} \right) = \nu \left( \frac{\partial^2 v}{\partial x^2} + \frac{\partial^2 v}{\partial y^2} + \frac{\partial^2 v}{\partial z^2} \right) - \frac{\partial p}{\partial y} + f_y \quad (3)$$

$$z: \rho \left( \frac{\partial w}{\partial t} + u \frac{\partial w}{\partial x} + v \frac{\partial w}{\partial y} + w \frac{\partial w}{\partial z} \right) = \nu \left( \frac{\partial^2 w}{\partial x^2} + \frac{\partial^2 w}{\partial y^2} + \frac{\partial^2 w}{\partial z^2} \right) - \frac{\partial p}{\partial z} + f_z \quad (4)$$

The computation's findings will eventually be used to calculate numerous parameters, including the Reynolds number. The Reynolds number is a numerical value that can determine whether a fluid flow is the laminar, transition, or turbulent. The Reynolds equation produces a dimensionless number representing the ratio of inertial to viscous forces [7]. The Reynolds number can be expressed using the Eq. (5)

$$Re = \frac{\rho v D}{\mu} \quad (5)$$

where Re is the Reynolds number,  $\rho$  is the fluid density ( $\text{kg/m}^3$ ), D is the diameter of the object (m),  $v$  is the fluid velocity (m/s), and  $\mu$  is the dynamic viscosity of the fluid (kg/ms). Increasing the Reynolds number will cause a fluid flow to become turbulent. One way to increase the Reynolds number is to accelerate the fluid flow [27]. The faster the fluid flows around the object, the greater the drag force [28]. Drag is the force that occurs on the object horizontally or in the direction of flowing fluid due to the distribution of pressure and friction around the object [2, 3]. This force is strongly influenced by the object's shape and the airflow's velocity. The existence of these forces produces a value known today as the drag coefficient ( $C_D$ ). The drag coefficient results will be displayed in the simulation in the form of a dimensionless graph that represents the truck's aerodynamic characteristics using the Eq. (6) [29]

$$C_D = \frac{F_D}{0.5 \rho A_s v^2} \quad (6)$$

where  $C_D$  is the coefficient drag,  $F_D$  is the drag force (N),  $\rho$  is the fluid density ( $\text{kg/m}^3$ ),  $A_s$  is the frontal area of the object ( $\text{m}^2$ ), and  $v$  is the fluid velocity (m/s).

#### 2.4 Domain and Boundary Conditions

Figure 3 shows the enclosure as the mesh domain in this simulation. In order to establish a control volume throughout the truck, the domain was made large than the model's; the objective of this size was to avoid the effect of the boundary layer on the domain wall [30]. According to Abdellah *et al.*,

[31], the domain dimensions could be created as follows:  $3L$  for the front length,  $5L$  for the back domain length, and  $3L$  for the top domain length, whereby  $L$  is the length of the truck. The inner box was created in the area surrounding the truck to control the mesh in the area side of the truck and observed the wake area behind truck [32].

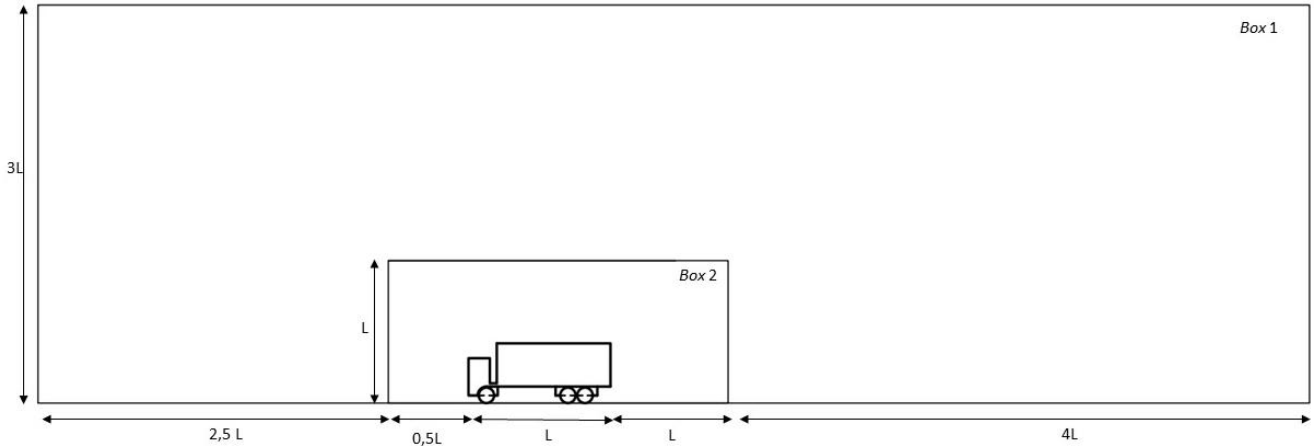


**Fig. 3.** Mesh domain in Ansys Fluent simulation

Table 2 depicts boundary conditions. The k-epsilon was used as the turbulence model, and the vehicle was considered moving at 30 m/s. This model was chosen because it is the most widely used turbulence model in solving hydrodynamic problems [33]. Moreover, the k-epsilon model is suitable for the application with a high Reynolds number; in this case, the Reynolds number was  $6.8 \times 10^6$ . Subsequently, k-epsilon is more accurate in modelling the complex flow detachment; thereby, this model would provide precise results to predict the drag coefficient on the car's body [34]. In the simulation, the truck geometry was symmetrical, assuming that both sides had the same flow pattern. This step aimed to reduce iteration time and simplify the mesh volume control.

**Table 2**

Boundary conditions and input value in Ansys Fluent

Boundary Conditions	Input Value
Inlet	Velocity inlet (30 m/s)
Outlet	Pressure outlet (0 Pa)
Symmetry side	Symmetry
The surface of the truck	Wall no slip
Outside and top side	Wall no slip

### 2.5 Grid Independence Test

One of the strategies used in CFD simulations to minimize numerical errors and remove unnecessary computational results is the grid independence test [35]. In incremental iterations, grid independence is achieved by increasing the number of meshes. The simulation results are presented as a graph that compares the simulation results to the number of grids or elements. The results of this simulation are used to choose the optimal refinement grid with a low error but a minimal number of meshes. In the CFD simulation, as much as possible, the simulation error is close to zero. This error reduction can be obtained by increasing the number of meshes. The simulation results will have a significant error when a large mesh size is used; however, a small mesh size will have a high level of

accuracy and make iterations run longer during the simulation process [36]. Table 3 shows the number of meshing elements utilized in the analysis to determine the error in simulation.

**Table 3**  
 Number of elements (grid)

No	Number of Elements
1	54,522
2	62,309
3	94,926
4	115,691
5	146,621
6	195,959
7	285,534
8	336,385

## 2.6 Fuel Consumption Analysis

A numerical study was conducted to compare fuel usage with the drag force created by the Ansys Fluent simulation. This comparison examines the fuel required to overcome the vehicle's drag. According to Praveen *et al.*, [5], the following equations can be used to express the relations between drag force and fuel consumption numerically

$$F_D = \frac{1}{2}(\rho A v^2 C_D) \tag{7}$$

$$P = F_D v \tag{8}$$

$$E = \frac{P}{V_{truck}} \tag{9}$$

$$F_C = \frac{E}{\phi d} \tag{10}$$

where  $F_D$  is the drag force (N),  $P$  is the power required to overcome drag (W),  $E$  is the energy consumption per kilometer-hour (Wh/km),  $V_{truck}$  is the truck speed (km/hour),  $F_C$  is the fuel consumption (L/km),  $v$  is the fluid velocity (m/s),  $\rho$  is the fluid density ( $1.225 \text{ kg/m}^3$ ),  $A$  is the frontal area of the vehicle ( $\text{m}^2$ ),  $C_D$  is the drag coefficient, and  $\phi d$  is the specific energy of the fuel (Wh/L). Truck fuel, specifically diesel with a specific energy of  $10.6 \times 10^3 \text{ Wh/L}$ , was used in this study [37].

## 3. Result and Discussions

### 3.1 Grid Independence Test

The grid independence test begins by converting a coarse mesh to a fine mesh. The mesh's results will be observed until the drag coefficient value does not change significantly. Figure 4 shows the relationship between the drag coefficient value and the number of elements at an airflow velocity of 30 m/s. The number of mesh elements 195,959, 285,534, and 336,385 has an insignificant change in the coefficient of drag with each drag coefficient value of 0.7701, 0.7729, and 0.7730. Considering the accuracy and time required for computation, a mesh with 195,959 elements was chosen for this simulation. Figure 5. depicts the meshed used in the simulation after selecting the proper mesh with the grid independence test.

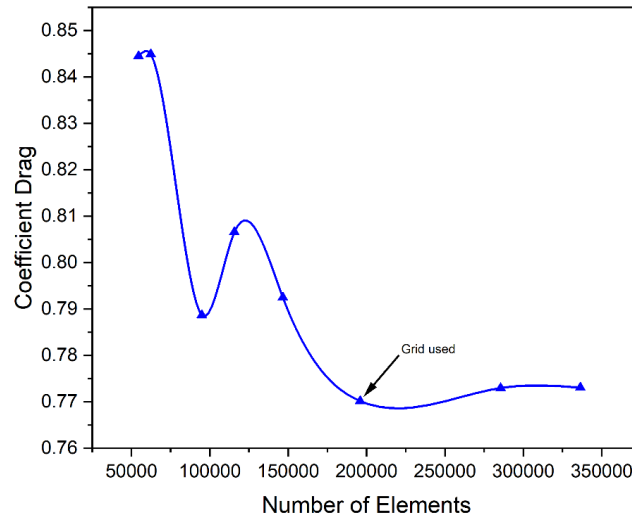


**Fig. 4.** Relationship between the drag coefficient and the number of elements in the grid independence test

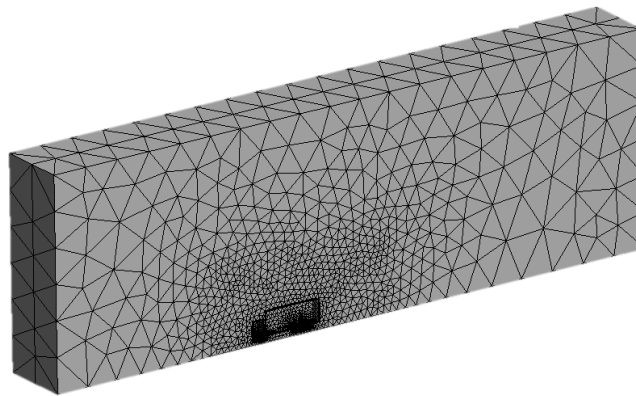


**Fig. 5.** The mesh used in the simulation

### 3.2 Drag Coefficient and Drag Force

Figure 6 depicts the result of the drag coefficient in the simulation. The results showed that the truck without adding a drag reduction device had the highest drag coefficient by 0.78. In contrast, the addition of a windshield as the drag reduction device tended to decrease the coefficient of drag to 0.67. Subsequently, the application of the cylinder as the drag reduction device also succeeded in reducing the truck coefficient drag. Compared with the truck without incorporating the drag reduction device, drag reduction type-cylinder, cylinder type-I, and cylinder type-D obtained lower drag coefficients by 0.76, 0.74, and 0.72, respectively. Among the cylinder drag reduction devices, cylinder type-D obtained the lowest drag coefficient by 7.69 %. According to Eq. (6), the drag coefficient would affect the truck's drag force. Figure 7 shows the drag force corresponding with the drag coefficient. The results showed that the highest drag force was 1511 N which occurred when the truck did not attach any drag reduction devices. To reduce the drag force, the addition of windshield, cylinder, cylinder type-I, and cylinder type-D decreased the drag force by 1309 N, 1475 N, 1442 N, and 1406 N, respectively. Therefore, these results validate the theory that the drag force decreases exponentially by reducing the drag coefficient.



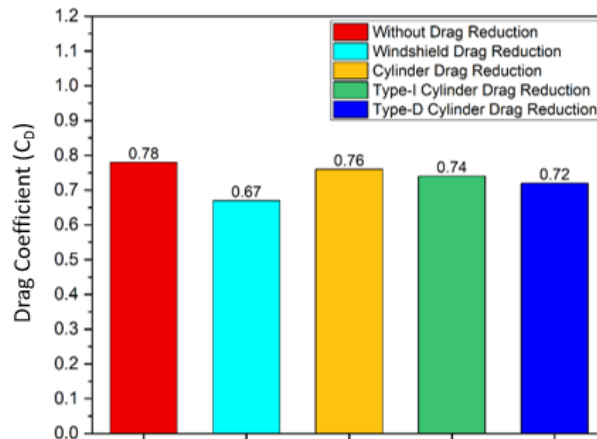


Fig. 6. Results of the drag coefficient in simulation

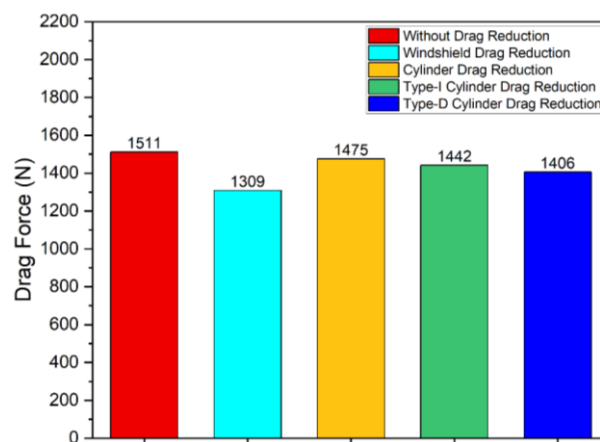
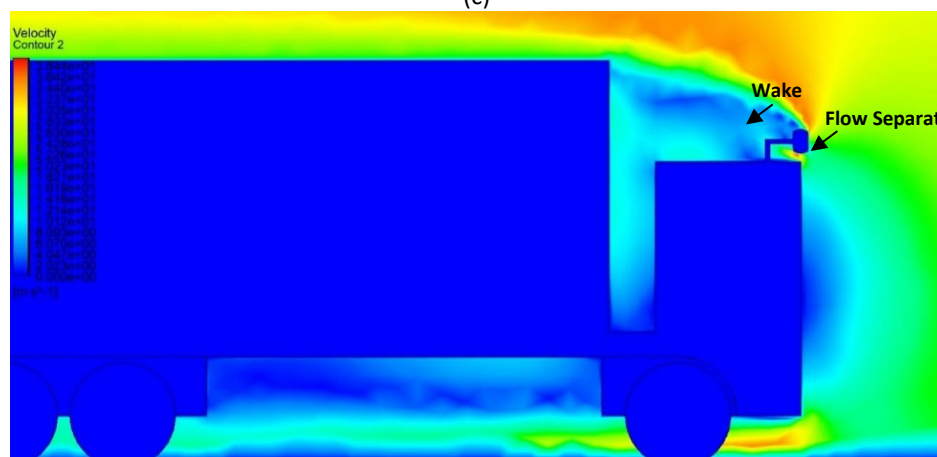
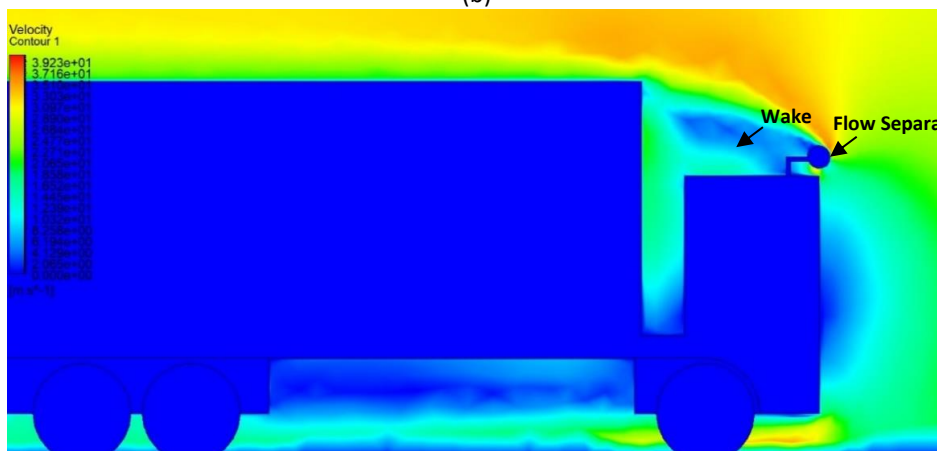
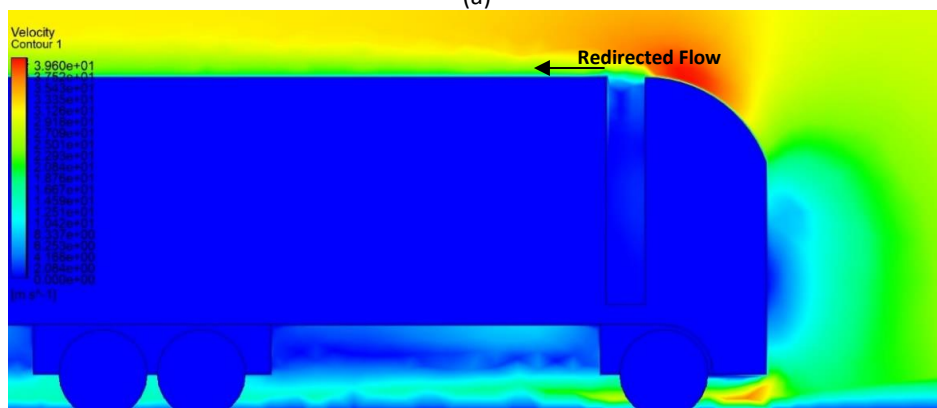
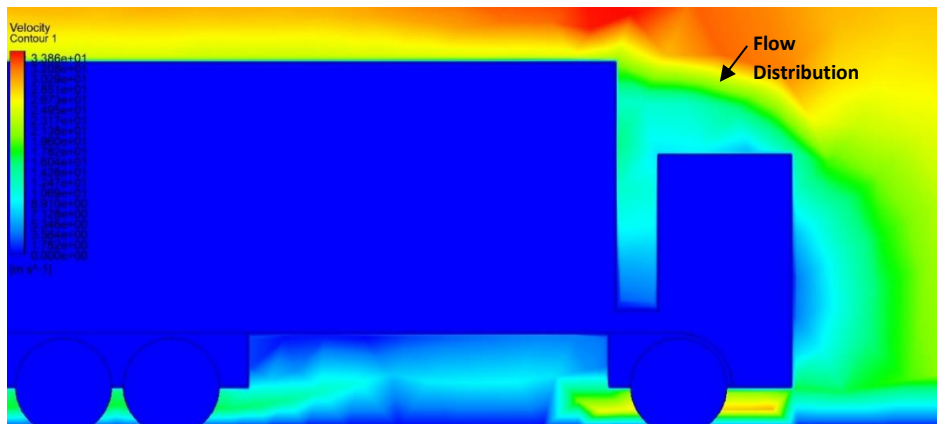
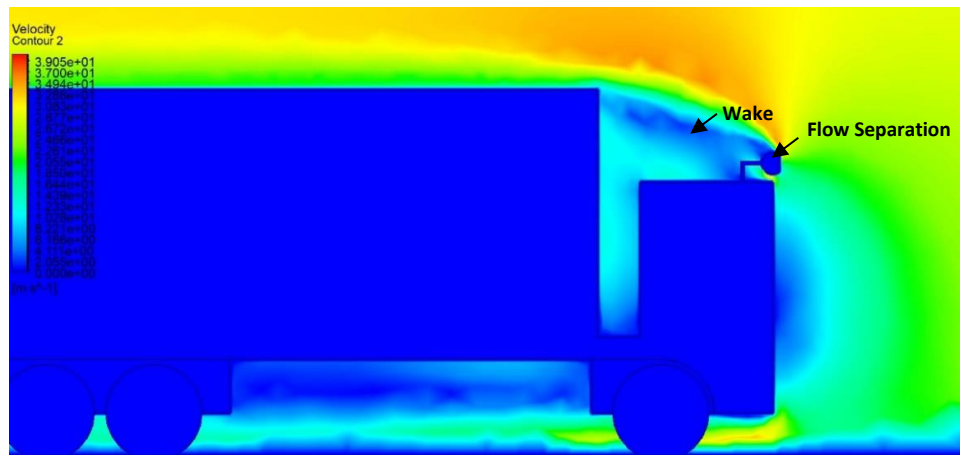


Fig. 7. Results of the drag force in simulation

### 3.3 Velocity Contour

To understand the underlying causes of the reduction of the drag force, the velocity contour on the truck was investigated. Figure 8 exhibits the visualization of velocity contour above the truck surface before the addition of a drag reduction device and after the addition of a drag reduction device. Figure 8(a) exhibits that the truck without the addition of the drag reduction device showed there was flow distribution above the truck; the visualization can be seen by the dominance of the light blue contour above the truck; thus, it was considered as the main cause of the increase in the drag force. Research by Hosravi *et al.*, [38] confirmed that when the truck did not use the drag reduction device, it contributed to the drag force increase because there would be high pressure on the truck surface. Figure 8(b) shows that adding the windshield drag reduction device could have decreased the drag coefficient at the truck because of the ability of the windshield to direct the air to flow above the truck surface. In the case of the cylinder drag reduction, Figure 8(c)-(e) show the difference between the velocity contour above the truck. It can be concluded that the application of cylinder type-D could have delayed the flow separation better than other cylinder devices. Figure 8(e) depicts the flow separation seen by the smaller wake region in the blue contour above the truck. The decrease of the coefficient of drag after adding a cylinder is caused by the increase of fluid flow velocity after the collision with cylinder devices; this phenomenon will increase the fluid momentum, leading to delayed flow separation because of the ability of the fluid to overcome the shear stress [10].





(e)

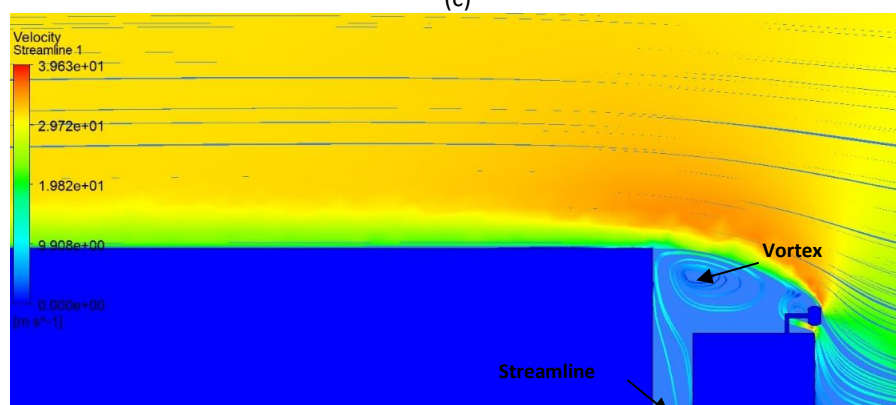
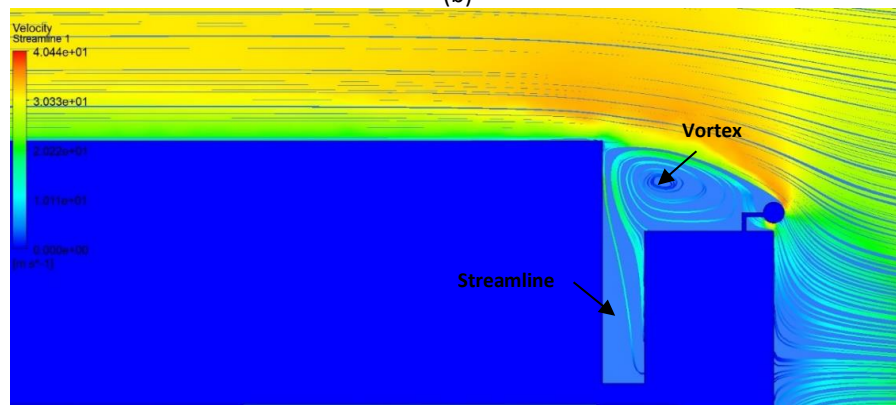
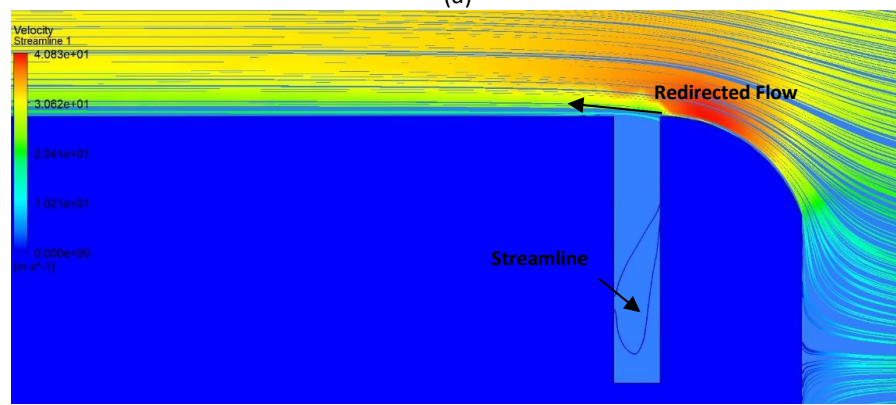
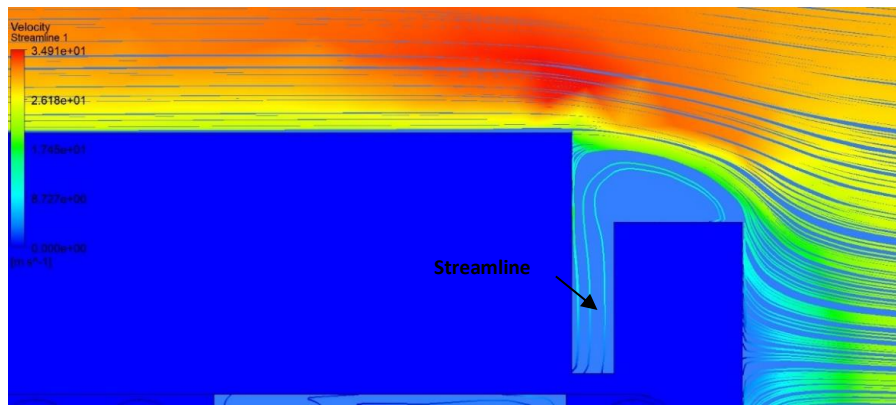
**Fig. 8.** Visualization of velocity contours on a truck, (a) Without drag reduction, (b) Windshield drag reduction, (c) Cylinder drag reduction, (d) Type-I drag reduction cylinder, (e) Type-D drag reduction cylinder

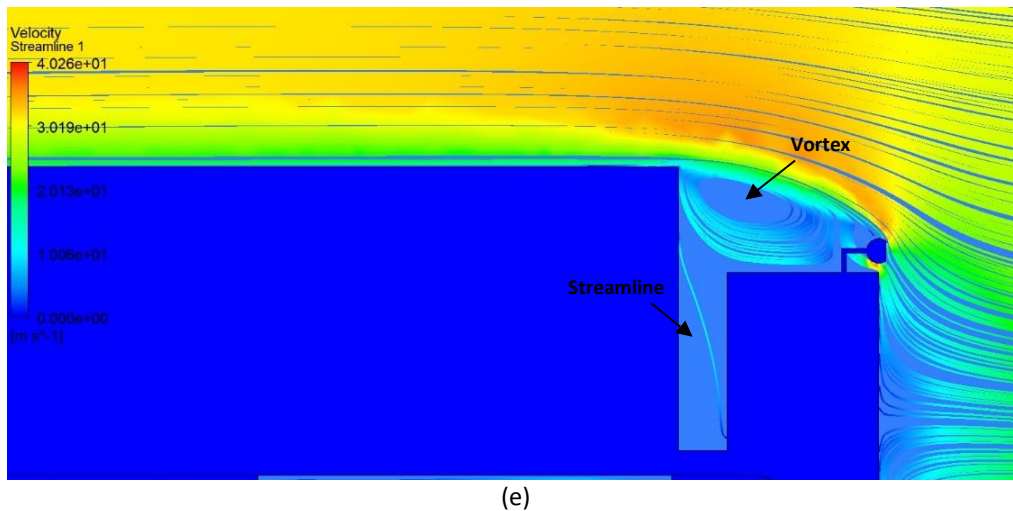
### 3.4 Velocity Streamline

The investigation of the velocity streamlines inside a gap between the truck and the container was conducted. Figure 9(a) shows that streamline without the drag reduction device after fluid crossed the truck front surface, there was streamline in the gap between truck and the container; the existence of the streamline could have affected the aerodynamic of the truck, caused an increase the truck drag coefficient [39]. Figure 9(b) depicts the truck streamline with the addition of the windshield, and the result showed that the streamline in the gap of the truck was reduced, which can be seen by the decrease of the velocity contour that had light blue color in the gap. Subsequently, the addition of the drag reduction cylinder type also made the variation streamline contour in the gap. Figure 9(c)-(e) shows that there was a reduction of streamline in the gap between truck and container; this phenomenon was assessed as one factor that contributed to the decrease of the coefficient of drag at the truck.

The velocity streamlines above the truck after the fluid crossed the drag reduction also had been studied. Figure 9(b) shows that the windshield's application could deprive the airflow circulation above the truck, and the windshield can direct the air to flow above the truck surface without any obstruction. This condition was assessed in the research conducted by Firman, *et al.*, [7], who reported that this flow condition would have affected the coefficient of drag of the truck. In addition, the streamlines change occurred when the truck was attached with cylinder-type drag reduction. Figures 9(c)-(e) show there was turbulent flow and vortex, which were formed behind the cylinder. The vortex formed after colliding with the cylinder can decrease the shear stress between the air and the truck surface.

Furthermore, this condition would have increased the fluid velocity afterward [40]. The difference in the vortex in the circulation zone behind the cylinder, cylinder type-I, and cylinder type-D was caused by the change of pressure distribution on the front surface of the truck. Therefore, it would have caused a delay in flow separation on the truck. This condition was confirmed by Yoon *et al.*, [41], who reported that the change of geometry angle would have delayed the flow separation and changed the vortex formation behind the geometry. In the case of the drag reduction cylinder type-D, the change of turbulence and vortex were contributed to direct the air to flow straight above the container truck. Figure 9(d) shows the flow with the light blue contour, which flows straight on the container surface after the vortex has been formed.





(e)  
**Fig. 9.** Streamline visualization on a truck, (a) Without drag reduction, (b) Windshield drag reduction, (c) Cylinder drag reduction, (d) Type-I drag reduction cylinder, and (e) Type-D drag reduction cylinder

### 3.5 The Reduction of Truck's Fuel Consumption

The truck's aerodynamics will affect the truck's fuel consumption, and the bigger the drag yielded by the truck will increase the fuel needed to drive the truck. Moreover, a study by Mokhtar *et al.*, [42] stated that every 2 % reduction in the drag force would have reduced 1 % fuel consumption. Thus, it is necessary to evaluate the influence of the drag reduction device on fuel consumption. From Eq. (10), the fuel consumption of trucks with various drag reduction devices can be investigated. Figure 10 shows the comparison of fuel consumption. According to the analysis, it can be stated that the use of the windshield can decrease fuel consumption by 13.37 % when compared with the truck without the drag reduction device. Adding a cylinder for drag reduction could also reduce the truck's fuel consumption by 2.38 %, 4.57 %, and 6.95 % for the drag reduction cylinder, cylinder type-I, and cylinder type-D, respectively. When the truck was attached with the cylinder type-D, the truck obtained the highest reduction in fuel consumption. These results also indicated that adding the drag reduction device to the truck would considerably increase fuel efficiency [43]. Therefore, it is essential to conduct further analysis in the addition of the drag reduction experimentally; thus, the proposed design can be applied in the future.

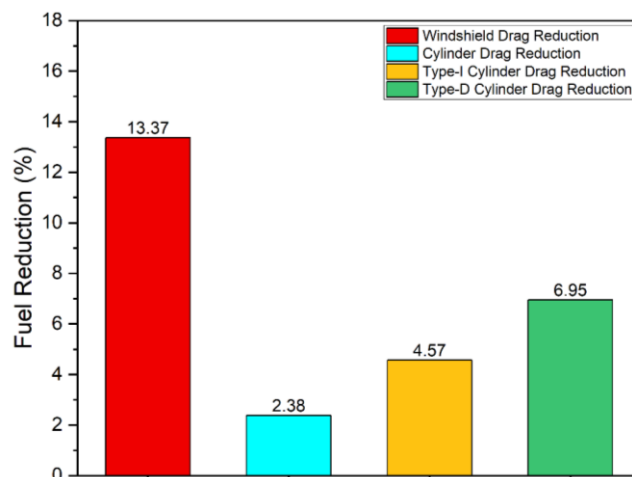


**Fig. 10.** Reduction of fuel consumption

## 4. Conclusions

According to the simulation results, it can be concluded that the reduction of the coefficient drag and the drag force can be predicted using computational methods. Therefore, using cylinder, cylinder type-I, and cylinder type-D as drag reduction devices could reduce the coefficient drag of the truck. The addition of round, type-I, and type-D cylinders formed turbulence and vortex, leading to the change of pressure distribution in the truck front surface. This condition could have delayed the flow separation point and caused the reduction of the drag force on the truck, with the highest reduction by using cylinder type-D. Although the computational methods state that there is a reduction in the coefficient drag, it is essential to conduct further analysis regarding the addition of the cylinder as the drag reduction device through experimental and theoretical methods, which further justified the results of this research. In addition, the reduction of the drag force and coefficient drag also contributed to the reduction in fuel consumption, with the highest fuel consumption reduction by using cylinder type-D.

## Acknowledgement

The authors wish to express our sincere gratitude to the Computer Laboratory at Mechanical Engineering Department, Udayana University, for providing us with the ANSYS 20.2 software that we used to run this simulation.

## References

- [1] Nath, Devang S., Prashant Chandra Pujari, Amit Jain, and Vikas Rastogi. "Drag reduction by application of aerodynamic devices in a race car." *Advances in Aerodynamics* 3, no. 1 (2021): 1-20. <https://doi.org/10.1186/s42774-020-00054-7>
- [2] Sudin, Mohd Nizam, Mohd Azman Abdullah, Shamsul Anuar Shamsuddin, Faiz Redza Ramli, and Musthafah Mohd Tahir. "Review of research on vehicles aerodynamic drag reduction methods." *International Journal of Mechanical and Mechatronics Engineering* 14, no. 02 (2014): 37-47.
- [3] Kamal, Muhammad Nabil Farhan, Izuan Amin Ishak, Nofrizalidris Darlis, Daniel Syafiq Baharol Maji, Safra Liyana Sukiman, Razlin Abd Rashid, and Muhamad Asri Azizul. "A review of aerodynamics influence on various car model geometry through CFD techniques." *Journal of Advanced Research in Fluid Mechanics and Thermal Sciences* 88, no. 1 (2021): 109-125. <https://doi.org/10.37934/arfmts.88.1.109125>
- [4] Vignesh, S., Vikas Shridhar Gangad, V. Jishnu, Amal Krishna, and Yagna S. Mukkamala. "Windscreen angle and Hood inclination optimization for drag reduction in cars." *Procedia Manufacturing* 30 (2019): 685-692. <https://doi.org/10.1016/j.promfg.2019.02.062>
- [5] Narendiranath Babu, T., Bandaru Shivasai, Vattikuti Mahesh, and Prashant Reddy. "Design and analysis of coconut fiber reinforced polyester composite leafspring." *International Journal of Mechanical Engineering and Technology* 8, no. 6 (2017): 544-552.
- [6] Landman, D., R. M. Wood, and W. S. Seay. "Understanding Practical Heavy Truck Drag Reduction Limits." *SAE Publication* (2009). <https://doi.org/10.4271/2009-01-2890>
- [7] Firman N, Habibie N, Ghurri A, Agung A, Suryawan A. "Simulasi Pengaruh Penambahan Headroof Spoiler Pada Truk Dengan Aplikasi CFD." *Jurnal Ilmiah Teknik Desain Mekanika* (2020): 9(3):998-1002.
- [8] Charles, Terrance, Zhiyin Yang, and Yiling Lu. "Assessment of Drag Reduction Devices Mounted on a Simplified Tractor-Trailer Truck Model." *Journal of Applied and Computational Mechanics* (2020).
- [9] Tsutsui, T., and T. Igarashi. "Drag reduction of a circular cylinder in an air-stream." *Journal of Wind Engineering and Industrial Aerodynamics* 90, no. 4-5 (2002): 527-541. [https://doi.org/10.1016/S0167-6105\(01\)00199-4](https://doi.org/10.1016/S0167-6105(01)00199-4)
- [10] Tista, Si Putu Gede Gunawan, and S. P. Gede. "Pengaruh Penempatan Penghalang Berbentuk Silinder Pada Posisi Vertikal Dengan Variasi Jarak Horisontal Di Depan Silinder Utama Terhadap Koefisien Drag." *Jurnal Ilmiah Teknik Mesin CakraM Vol 4*, no. 2 (2010): 160-165.
- [11] Widodo, Wawan Aries, and Nuzul Hidayat. "Experimental study of drag reduction on circular cylinder and reduction of pressure drop in narrow channels by using a cylinder disturbance body." In *Applied Mechanics and Materials*, vol. 493, pp. 198-203. Trans Tech Publications Ltd, 2014. <https://doi.org/10.4028/www.scientific.net/AMM.493.198>

- [12] Triyogi, Y., D. Suprayogi, and E. Spirda. "Reducing the drag on a circular cylinder by upstream installation of an I-type bluff body as passive control." *Proceedings of the Institution of Mechanical Engineers, Part C: Journal of Mechanical Engineering Science* 223, no. 10 (2009): 2291-2296. <https://doi.org/10.1243/09544062JMES1543>
- [13] Siddharth Jena, Ajay Gairola. "Development of Computational Benchmarking Model for Infusion Pumps", *Journal of Advanced Research in Experimental Fluid Mechanics and Heat Transfer* (2022): 7 (1): 1-15.
- [14] Abdulhafid M A Elfaghi, Alhadi A Abosbaia, Munir F A Alkbir, Abdoulhdi A B Omran. "CFD Simulation of Forced Convection Heat Transfer Enhancement in Pipe Using Al<sub>2</sub>O<sub>3</sub>/Water Nanofluid", *Journal of Advanced Research in Micro and Nano Engineering* (2022): 7 (1): 8-13.
- [15] Abdulhafid M. A. Elfaghi, Alhadi A. Abosbaia, Munir F. A. Alkbir, Abdoulhdi A. B. Omran. "CFD Simulation of Forced Convection Heat Transfer Enhancement in Pipe Using Al<sub>2</sub>O<sub>3</sub>/Water Nanofluid", *Journal of Advanced Research in Numerical Heat Transfer* (2022): 8 (1): 44-49.
- [16] Liang, Chua Bing, Akmal Nizam Mohammed, Azwan Sapit, Mohd Azahari Razali, Mohd Faisal Hushim, Amir Khalid, and Nurul Farhana Mohd Yusof. "Numerical simulation of aerofoil with flow injection at the upper surface." (2021).
- [17] Sajali, Muhammad Fahmi Mohd, Abdul Aabid, Sher Afghan Khan, Fharukh Ahmed Ghasi Mehaboobali, and Erwin Sulaeman. "Numerical investigation of flow field of a non-circular cylinder." (2021).
- [18] Bajuri, Muhammad Nur Arham, Djamal Hissein Didane, Mahamat Issa Boukhari, and Bukhari Manshoor. "Computational Fluid Dynamics (CFD) Analysis of Different Sizes of Savonius Rotor Wind Turbine." *Journal of Advanced Research in Applied Mechanics* 94, no. 1 (2022): 7-12. <https://doi.org/10.37934/aram.94.1.712>
- [19] Ismail, Muhammad Pirdaus, Izuan Amin Ishak, Nor Afzanizam Samiran, Ahmad Faiz Mohammad, Zuliazura Mohd Salleh, and Nofrizalidris Darlis. "CFD Analysis on the Effect of Vortex Generator on Sedan Car using ANSYS Software." *International Journal of Integrated Engineering* 14, no. 1 (2022): 73-83.
- [20] Kamal, Muhammad Nabil Farhan, Izuan Amin Ishak, Nofrizalidris Darlis, Nurshafinaz Mohd Maruai, Rahim Jamian, Razlin Abd Rashid, NorAfzanizam Samiran, and Nik Normunira Mat Hassan. "Flow Structure Characteristics of the Simplified Compact Car Exposed to Crosswind Effects using CFD." *Journal of Advanced Research in Applied Sciences and Engineering Technology* 28, no. 1 (2022): 56-66. <https://doi.org/10.37934/araset.28.1.5666>
- [21] Tan, Nurfarah Diana Mohd Ridzuan, Fudhail Abdul Munir, Musthafah Mohd Tahir, Nurfarah Nabila Saad Azam, and Herman Saputro. "Effect of Dielectric Barrier Discharge (DBD) Plasma Actuator on Aerodynamics Performance of Vehicle Spoiler." In *Proceedings of the 7th International Conference and Exhibition on Sustainable Energy and Advanced Materials (ICE-SEAM 2021), Melaka, Malaysia*, pp. 430-433. Singapore: Springer Nature Singapore, 2022. [https://doi.org/10.1007/978-981-19-3179-6\\_81](https://doi.org/10.1007/978-981-19-3179-6_81)
- [22] Abidin, Harris Fadzillah Zainal, Md Tasyrif Abdul Rahman, Abdul Hamid Adom, Mohd Ridzuan Mohd Jamir, Sufi Suraya Halim, and Mohd Al Hafiz Mohd Nawi. "An Analysis of Urban Vehicle Body Aerodynamics Using Computational Fluid Dynamics for the Shell Eco-Marathon Challenge." *Journal of Advanced Research in Applied Sciences and Engineering Technology* 30, no. 2 (2023): 75-91. <https://doi.org/10.37934/araset.30.2.7591>
- [23] Kamal, Muhammad Nabil Farhan, Izuan Amin Ishak, Nofrizalidris Darlis, Nurshafinaz Mohd Maruai, Rahim Jamian, Razlin Abd Rashid, NorAfzanizam Samiran, and Nik Normunira Mat Hassan. "Flow Structure Characteristics of the Simplified Compact Car Exposed to Crosswind Effects using CFD." *Journal of Advanced Research in Applied Sciences and Engineering Technology* 28, no. 1 (2022): 56-66. <https://doi.org/10.37934/araset.28.1.5666>
- [24] Igarashi, Tamotsu, and Yoshihiko Shiba. "Drag reduction for D-shape and I-shape cylinders (Aerodynamic mechanism of reduction of drag)." *JSME International Journal Series B Fluids and Thermal Engineering* 49, no. 4 (2006): 1036-1042. <https://doi.org/10.1299/jsmeb.49.1036>
- [25] Chen, Xiaolin, and Yijun Liu. *Finite element modeling and simulation with ANSYS Workbench*. CRC press, 2018. <https://doi.org/10.1201/9781351045872>
- [26] ANSYS, Inc. "ANSYS FLUENT theory guide: Release 16.2." ANSYS, Canonsburg, Pennsylvania (2013).
- [27] Cimbala, John M., and Yunus A. Cengel. *Fluid mechanics: fundamentals and applications*. McGraw-Hill Higher Education, 2006.
- [28] Saint-Michel, Brice, Bérengère Dubrulle, Louis Marié, Florent Ravelet, and François Daviaud. "Influence of Reynolds number and forcing type in a turbulent von Kármán flow." *New Journal of Physics* 16, no. 6 (2014): 063037. <https://doi.org/10.1088/1367-2630/16/6/063037>
- [29] Markina, A. A., A. D. Lukashuk, S. N. Chepkasov, and A. V. Starovoytenko. "Improving aerodynamic characteristics for drag reduction of heavy truck." In *IOP Conference Series: Materials Science and Engineering*, vol. 862, no. 3, p. 032032. IOP Publishing, 2020. <https://doi.org/10.1088/1757-899X/862/3/032032>
- [30] Ilmi, Syamsuri, Zain Lillahulhaq, and M. Yusron. "Simulation of Fluid Flow Through Sedan Car YRS 4 Doors with Speed Variation using CFD." *Jurnal Rekayasa Mesin* 11, no. 3 (2020): 395-400. <https://doi.org/10.21776/ub.jrm.2020.011.03.11>

- [31] Al-Saadi, A., A. Hassanpour, and T. Mahmud. "Simulations of aerodynamic behaviour of a super utility vehicle using computational fluid dynamics." *Adv. Automob. Eng* 5, no. 134 (2016): 1-5. <https://doi.org/10.4172/2167-7670.1000134>
- [32] Abdellah, Essaghour, and Bo Wang. "CFD analysis on effect of front windshield angle on aerodynamic drag." In *IOP Conference Series: Materials Science and Engineering*, vol. 231, no. 1, p. 012173. IOP Publishing, 2017. <https://doi.org/10.1088/1757-899X/231/1/012173>
- [33] Ait Moussa, Abdellah, Justin Fischer, and Rohan Yadav. "Aerodynamic drag reduction for a generic truck using geometrically optimized rear cabin bumps." *Journal of Engineering* 2015 (2015). <https://doi.org/10.1155/2015/789475>
- [34] Fathuddiin, Abubakar, and Samuel Samuel. "Meshing strategi untuk memprediksi hambatan total pada kapal planing hull." *Jurnal Rekayasa Mesin* 12, no. 2 (2021): 381-390. <https://doi.org/10.21776/ub.jrm.2021.012.02.15>
- [35] Hughes, Thomas. "CFD Study of Flow over a Simplified Car Using Different Turbulence Models." *PhD diss., University of Derby* (2018).
- [36] Charles, Terrance, Zhiyin Yang, and Yiling Lu. "Assessment of Drag Reduction Devices Mounted on a Simplified Tractor-Trailer Truck Model." *Journal of Applied and Computational Mechanics* (2020).
- [37] Humphreys, Hugh Luke, Joshua Batterson, David Bevely, and Raymond Schubert. *An evaluation of the fuel economy benefits of a driver assistive truck platooning prototype using simulation*. No. 2016-01-0167. SAE Technical Paper, 2016. <https://doi.org/10.4271/2016-01-0167>
- [38] Giddings, J., R. Lake, and C. Matthews. "Comparing running costs of diesel, LPG and electrical pumpsets." *Primefact 1419 First Edition DPI Agriculture Water and Irrigation Unit* (2016): 1-4.
- [39] Khosravi, Mehrdad, Farshid Mosaddeghi, Majid Oveisi, and Ali khodayari-b. "Aerodynamic drag reduction of heavy vehicles using append devices by CFD analysis." *Journal of Central South University* 22 (2015): 4645-4652. <https://doi.org/10.1007/s11771-015-3015-7>
- [40] Hariram, Adithya, Thorsten Koch, Björn Mårdberg, and Jan Kyncl. "A study in options to improve aerodynamic profile of heavy-duty vehicles in Europe." *Sustainability* 11, no. 19 (2019): 5519. <https://doi.org/10.3390/su11195519>
- [41] Peng, Jing, Tie Wang, Tiantian Yang, Xiuquan Sun, and Guoxing Li. "Research on the aerodynamic characteristics of tractor-trailers with a parametric cab design." *Applied Sciences* 8, no. 5 (2018): 791. <https://doi.org/10.3390/app8050791>
- [42] Yoon, Dong-Hyeog, Kyung-Soo Yang, and Choon-Bum Choi. "Flow past a square cylinder with an angle of incidence." *Physics of fluids* 22, no. 4 (2010): 043603. <https://doi.org/10.1063/1.3388857>
- [43] Mokhtar, Wael, Kyle Dinger, Shardul Kachare, M. Hossain, and Colin Britcher. "A CFD Study Investigating Drag Reduction for Different Offset and Inline Distance for Two Trucks Platooning." *J. Energy Power Eng* 14 (2020): 143-150. <https://doi.org/10.17265/1934-8975/2020.05.001>
- [44] Roy, Subrata, and Pradeep Srinivasan. "External flow analysis of a truck for drag reduction." *SAE transactions* (2000): 808-812. <https://doi.org/10.4271/2000-01-3500>